CD44 is required for the pathogenesis of experimental crescentic glomerulonephritis and collapsing focal segment....

Article *in* Kidney International · December 2017

DOI: 10.1016/j.kint.2017.09.020

CITATIONS
0

READS
26

16 authors, including:

Jennifer Eymael
Radboud University Medical Centre (Radbou...
3 PUBLICATIONS **1** CITATION
SEE PROFILE

Shagun Khera
University of Plymouth
8 PUBLICATIONS **107** CITATIONS
SEE PROFILE

Markus A Loeven
Radboud University Medical Centre (Radbou...
10 PUBLICATIONS **30** CITATIONS
SEE PROFILE

CD44 is required for the pathogenesis of experimental crescentic glomerulonephritis and collapsing focal segmental glomerulosclerosis

Jennifer Eymael[1,7], Shagun Sharma[2,3,7], Markus A. Loeven[2], Jack F. Wetzels[2], Fieke Mooren[1], Sandrine Florquin[4], Jeroen K. Deegens[2], Brigith K. Willemsen[1], Vikram Sharma[2,3], Toin H. van Kuppevelt[5], Marinka A. Bakker[2], Tammo Ostendorf[6], Marcus J. Moeller[6], Henry B. Dijkman[1], Bart Smeets[1,7] and Johan van der Vlag[2,7]

[1]Department of Pathology, RIMLS, RIHS, Radboud University Medical Center, Nijmegen, The Netherlands; [2]Department of Nephrology, RIMLS, RIHS, Radboud University Medical Center, Nijmegen, The Netherlands; [3]School of Biomedical and Healthcare Sciences, Plymouth University, Plymouth, UK; [4]Department of Pathology, Academic Medical Center, Amsterdam, The Netherlands; [5]Department of Biochemistry, RIMLS, RIHS, Radboud University Medical Center, Nijmegen, The Netherlands; and [6]Division of Nephrology and Clinical Immunology, RWTH University of Aachen, Aachen, Germany

A key feature of glomerular diseases such as crescentic glomerulonephritis and focal segmental glomerulosclerosis is the activation, migration and proliferation of parietal epithelial cells. CD44-positive activated parietal epithelial cells have been identified in proliferative cellular lesions in glomerular disease. However, it remains unknown whether CD44-positive parietal epithelial cells contribute to the pathogenesis of scarring glomerular diseases. Here, we evaluated this in experimental crescentic glomerulonephritis and the transgenic anti-*Thy1.1* model for collapsing focal segmental glomerulosclerosis in CD44-deficient (*cd44-/-*) and wild type mice. For both models albuminuria was significantly lower in *cd44-/-* compared to wild type mice. The number of glomerular Ki67-positive proliferating cells was significantly reduced in *cd44-/-* compared to wild type mice, which was associated with a reduced number of glomerular lesions in crescentic glomerulonephritis. In collapsing focal segmental glomerulosclerosis, the extracapillary proliferative cellular lesions were smaller in *cd44-/-* mice, but the number of glomerular lesions was not different compared to wild type mice. For crescentic glomerulonephritis the influx of granulocytes and macrophages into the glomerulus was similar. *In vitro*, the growth of CD44-deficient murine parietal epithelial cells was reduced compared to wild type parietal epithelial cells, and human parietal epithelial cell migration could be inhibited using antibodies directed against CD44. Thus, CD44-positive proliferating glomerular cells, most likely parietal epithelial cells, are essential in the pathogenesis of scarring glomerular disease.

Kidney International (2018) ■, ■–■; https://doi.org/10.1016/j.kint.2017.09.020

KEYWORDS: CD44; cell migration; collapsing FSGS; crescentic glomerulonephritis; parietal epithelial cells

Parietal epithelial cells (PECs) line the Bowman capsule of a healthy glomerulus. Like podocytes, PECs have the same embryonic origin.[1,2] Unlike podocytes, PECs retain the ability to proliferate, which occurs under pathologic conditions.[3,4] In adult kidney, various subpopulations of PECs have been described, such as parietal podocytes,[5–7] adult parietal epithelial multipotent progenitors,[8,9] and activated PECs,[4,10,11] with some variation among species. Activated PECs are known mainly for their involvement in the development of hyperplastic lesions in focal and segmental glomerulosclerosis (FSGS) and crescentic glomerulonephritis.[10,12]

Extracapillary proliferative lesions or crescents are the hallmark of both inflammatory and noninflammatory glomerular diseases. In fact, lesion formation or glomerular scarring is responsible for the irreversible loss of renal function in most glomerular diseases. Evidence indicates that the extracapillary proliferative cellular lesions in (experimental) crescentic glomerulonephritis and collapsing focal and segmental glomerulosclerosis (FSGS) are composed mainly of activated PECs.[4,10] In experimental collapsing FSGS, induced damage to podocytes triggers the activation of PECs followed by the formation of adhesions and invasion by PECs of the glomerular tuft. The migrating and proliferating activated PECs deposit extracellular matrix material, which accumulates over time, resulting in segmental, and ultimately global, scarring of the glomerular tuft.[10,12] In experimental crescentic glomerulonephritis, anti-glomerular basement membrane

Correspondence: *Johan van der Vlag, Department of Nephrology (480), RIMLS, RIHS, Radboud University Medical Centre, Geert Grooteplein 10, 6525 GA Nijmegen, The Netherlands. E-mail: Johan.vanderVlag@radboudumc.nl or Bart Smeets, Department of Pathology (824), RIMLS, RIHS, Radboud University Medical Centre, Geert Grooteplein 24, 6525 GA Nijmegen, The Netherlands. E-mail: Bart.Smeets@radboudumc.nl*

[7]JE, SS, BS, and JvdV contributed equally to this article.

Received 2 April 2017; revised 11 September 2017; accepted 21 September 2017

(anti-GBM) antibodies, eventually in conjunction with toll-like-receptor (TLR) ligands, lead to activation of the complement system and glomerular influx of inflammatory cells, such as granulocytes and macrophages.[13–15] Simultaneously, PECs, and to a lesser extent podocytes, are activated, thereby generating proliferative cellular lesions and the typical crescents, which may block the tubular outlet and urinary flow.[4]

The proliferative cells within sclerotic lesions have been identified as activated PECs in human biopsies of a range of glomerular diseases as well.[11,16–21] Based on the aforementioned animal and human studies, activation of PECs has been proposed as a common mechanism in crescentic glomerulonephritis and primary and secondary FSGS.[12,22]

Activated PECs can be identified by an acquired expression of cluster of differentiation 44 (CD44), which is a cell surface glycoprotein that plays a key role in various cellular processes, such as cell differentiation, cell migration, cell-matrix binding, leukocyte trafficking, and scar formation.[23] Normally, CD44 is not expressed in a healthy glomerulus, but CD44 expression by proliferating PECs is higher in crescents and lesions in the presence of crescentic glomerulonephritis and FSGS.[11,24–26] The specific pattern of CD44 expression on activated PECs may suggest that CD44 expression by PECs contributes to the pathogenesis of scarring glomerular diseases. However, whether the acquired CD44 expression by activated PECs is a cause or consequence of glomerular scarring is not clear. In the current study, we evaluated the role of CD44 in experimental crescentic glomerulonephritis and FSGS, which revealed that CD44 is required for the pathogenesis of these scarring glomerular diseases.

RESULTS

CD44 deficiency reduces glomerular fibrinogen deposition and albuminuria in crescentic glomerulonephritis

To evaluate the role of CD44 in scarring glomerular diseases, we induced crescentic glomerulonephritis in wild-type (WT) and CD44-deficient (*cd44–/–*) mice and analyzed these mice at day 14. WT mice injected with saline showed no renal CD44 expression (Figure 1a), whereas nephrotoxic serum (NTS)–injected WT mice acquired glomerular, peri-glomerular, and tubular CD44 expression (Figure 1b and e). As expected, NTS-injected *cd44–/–* mice displayed no renal CD44 expression (Figure 1c, d, and f). To assess whether CD44 deficiency results in a kidney phenotype, we examined the histology and presence of granulocytes, macrophages, B cells, and T cells in normal, i.e., non-treated, WT and *cd44–/–* mice. Both types of mice had a normal renal histology (Supplementary Figure S1), and no differences were observed in the number of immune cells within the kidney (data not shown).

To exclude the possibility that CD44 deficiency affects the binding of the sheep anti-GBM serum, we stained for sheep Ig and found a similar appearance for WT and *cd44–/–* mice

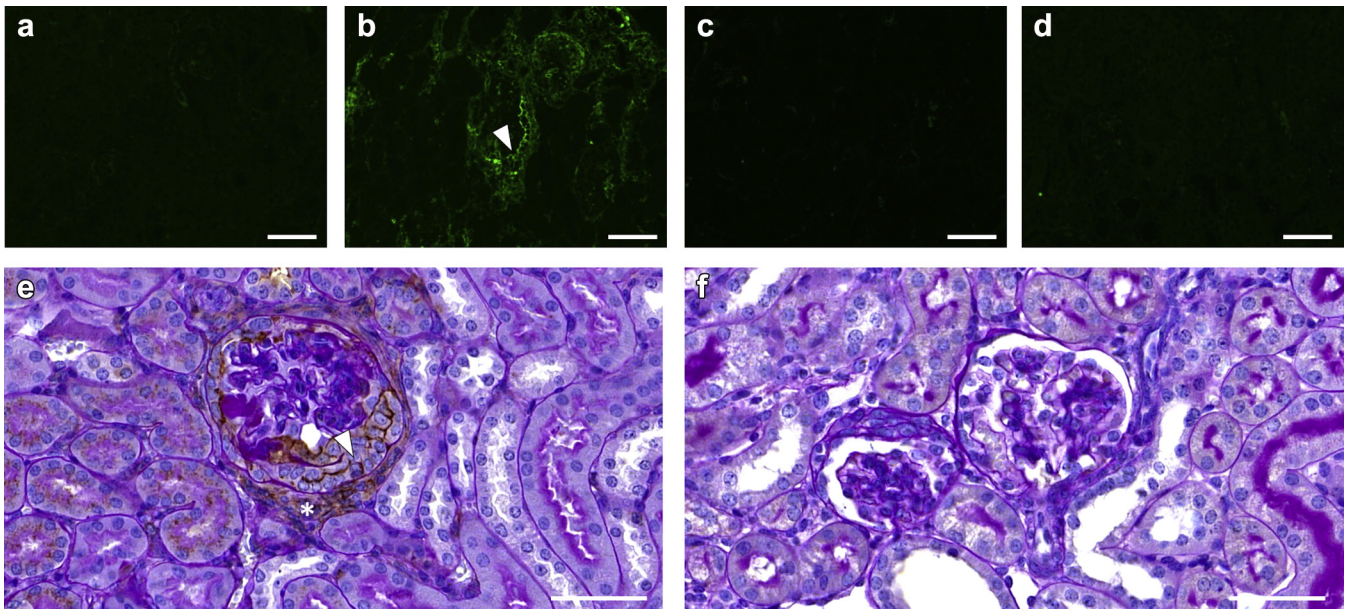

Figure 1 | Confirmation of CD44 deficiency in cd44–/– mice. To confirm cluster of differentiation 44 (CD44) deficiency in *cd44–/–* mice, renal cryosections were stained with anti-CD44 antibody 14 days after nephrotoxic serum (NTS) injection, versus controls. Shown are the following: wild-type (WT) mouse injected with saline only (**a**); WT mouse injected with NTS (**b**); *cd44–/–* mouse after NTS injection (**c**); and secondary antibody control (**d**). Only in the WT mouse injected with NTS was a *de novo* expression of CD44 detected (**b**, arrowhead). Bar = 100 μm. Immunostaining for CD44 on a kidney section stained with periodic acid–Schiff of an NTS-injected WT (**e**) and a *cd44–/–* mouse (**f**), respectively. Only in the WT mouse CD44 immunostaining was detected in the epithelial cells of affected glomeruli and in the peri-glomerular area (asterisks). Bar = 50 μm. To optimize viewing of this image, please see the online version of this article at www.kidney-international.org.

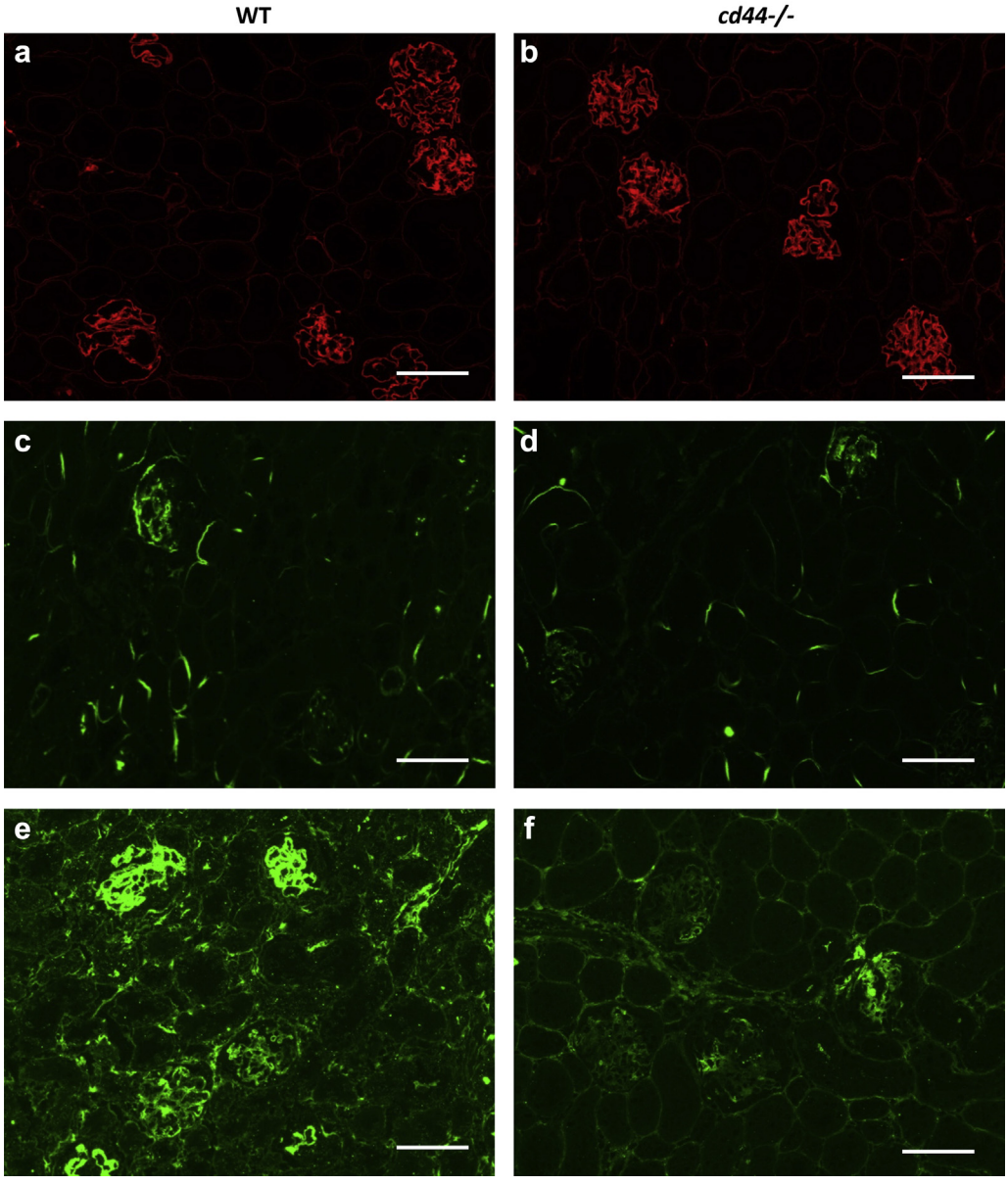

Figure 2 | Reduced fibrinogen deposition in *cd44–/–* mice. Effect of cluster of differentiation 44 (CD44) deficiency on nephrotoxic serum (NTS) antibody binding and complement C3c and fibrinogen deposition in glomeruli. Immunostaining using anti-sheep Alexa 594 conjugated secondary antibody 14 days after injection to compare sheep IgG binding to the glomerular basement membrane of wild-type (WT) (**a**) and *cd44–/–* mice (**b**). Complement C3c deposition in the glomeruli of NTS-injected WT (**c**) and *cd44–/–* mice (**d**). Fibrinogen deposition in the glomeruli of NTS-injected WT (**e**) and *cd44–/–* mice (**f**). Bar = 100 μm. To optimize viewing of this image, please see the online version of this article at www.kidney-international.org.

(Figure 2a and b). In accordance with equal glomerular Ig binding, glomerular complement factor C3c deposition was found to be similar in WT and *cd44–/–* mice (Figure 2c and d). Glomerular fibrinogen deposition, an important mediator in crescentic glomerulonephritis,[27] was markedly reduced in *cd44–/–* mice, compared with WT mice (Figure 2e and f).

The urinary albumin:creatinine ratio of *cd44–/–* mice was 4-fold lower, compared with that in WT mice (Figure 3a). Renal function did not differ between NTS-injected WT and *cd44–/–* mice, which had respective blood urea nitrogen values of 15.1 ± 1.2 versus 17.1 ± 1.9 mmol/l, compared with 12.1 ± 0.6 mmol/l for saline-injected controls.

CD44 deficiency reduces glomerular injury and glomerular cell proliferation in crescentic glomerulonephritis

Analysis of renal histology showed about 2-fold less affected glomeruli (~20% vs. ~50%) in NTS-injected *cd44–/–* mice, compared with WT mice (Figure 3b). In particular, *cd44–/–* mice (Figure 3d and f) displayed less crescent formation compared with WT mice (Figure 3c and e).

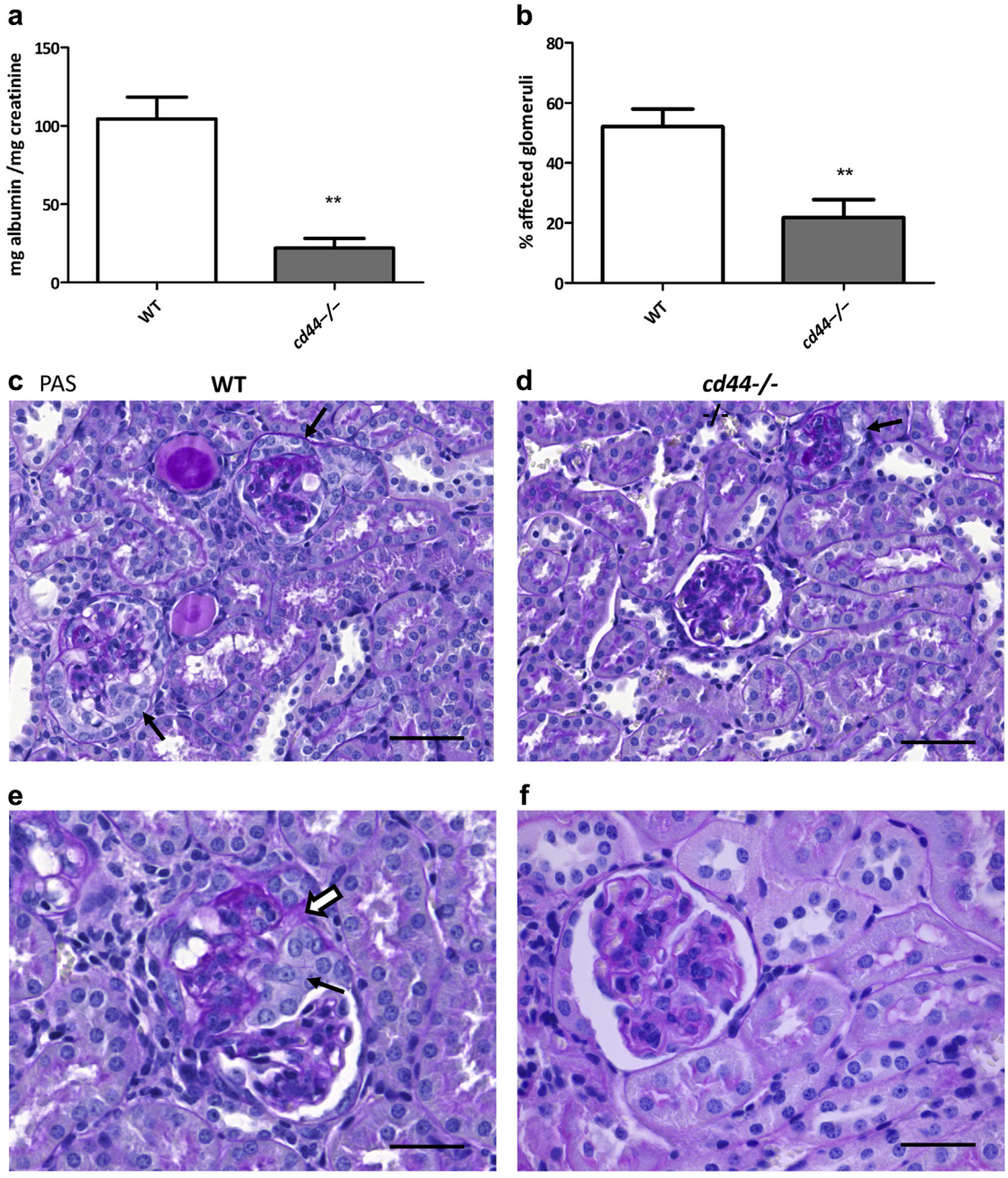

Figure 3 | Reduced proteinuria and crescent formation in cluster of differentiation 44–deficient (*cd44–/–*) mice. Proteinuria expressed as mg albumin/mg creatinine ratio in wild-type (WT) and *cd44–/–* mice on day 14 after nephrotoxic serum (NTS) injection (**a**). The formation of crescents or hyalinosis in the glomeruli was determined by analysis of at least 50 glomeruli per mouse and expressed as the percentage of affected glomeruli in WT and *cd44–/–* mice on day 14 after NTS injection (**b**). Data are given as mean ± SEM (n = 5). Mann Whitney U test (2-tailed); $^{**}P < 0.01$. Representative images of sections stained with periodic acid–Schiff of WT control mice (**c,e**) and *cd44–/–* mice (**d,f**). Bar = 100 μm (**c,d**) and 50 μm (**e,f**). Hyperplasia or multilayered accumulation of cells forming (pseudo)-crescents (**c,d,e**, arrows) and deposition of extracellular matrix between the cellular layers (**e**, open arrow) are depicted. To optimize viewing of this image, please see the online version of this article at www.kidney-international.org.

Given that we observed hyperplasia resulting in multilayers of cells in Bowman space and an occasional mitotic body, indicating cell proliferation, we next analyzed glomerular cell proliferation, which may contribute to the formation of crescents. A count of the number of Ki67-positive cells in both the glomerular tuft and Bowman space showed, for both compartments, about 2-fold fewer proliferating cells in *cd44–/–* mice, compared with WT mice, whereas the differences in Bowman space seemed more pronounced (Figure 4a–d).

Fewer PECs in crescentic lesions in cd44–/– mice

To examine the presence of activated PECs, we stained for PEC markers SSeCKS and claudin-1, and for CD44. As illustrated in

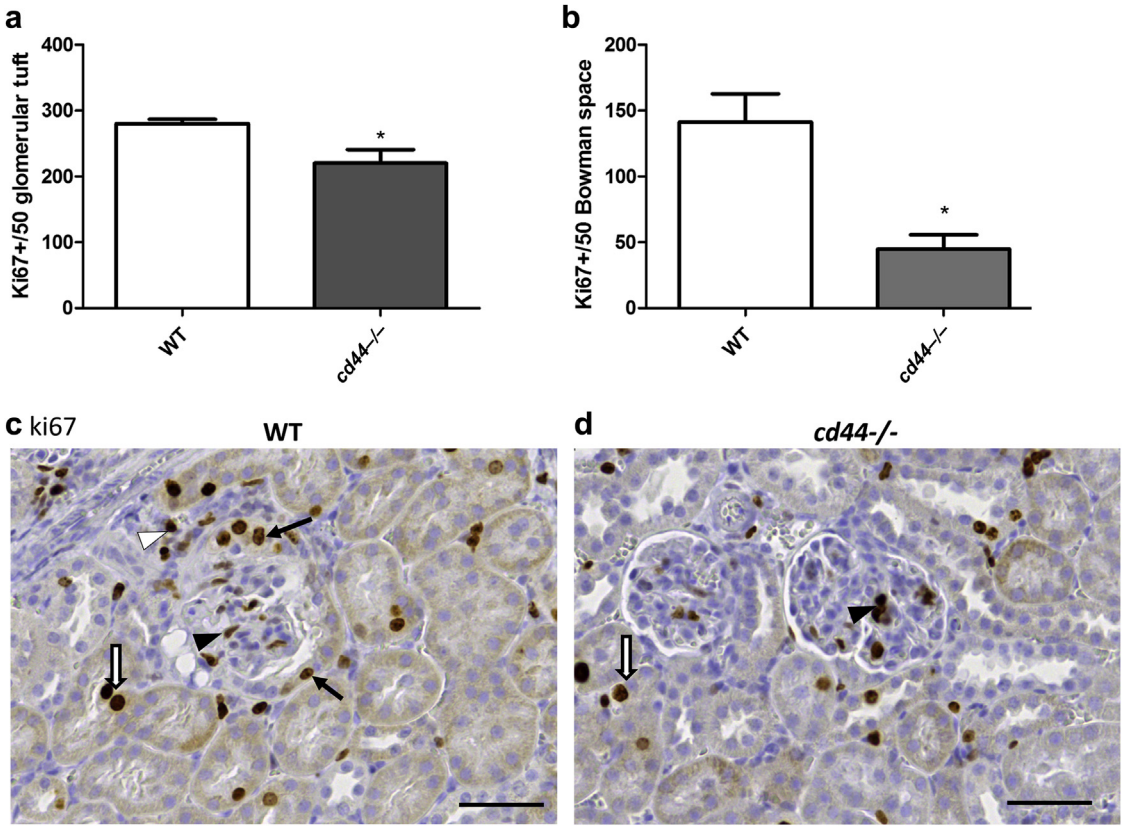

Figure 4 | Reduced proliferation of glomerular cells in cluster of differentiation 44–deficient (*cd44–/–*) mice. The number of Ki67-positive cells located in the glomerular tuft (**a**) and Bowman space (**b**) was counted in 50 glomeruli of wild-type (WT) and *cd44–/–* mice on 3,3′-diaminobenzidine–stained formalin-fixed paraffin sections (**c,d**). Data are given as mean ± SEM for WT (n = 5) and *cd44–/–* (n = 5) mice. Mann-Whitney U test (2-tailed); $^*P < 0.05$. Representative image showing Ki67 positive cells 14 days after nephrotoxic serum injection in WT (**c**) and *cd44–/–* mice (**d**). Cells positive for Ki67 were detected in the glomerular tuft (black arrowheads), Bowman space (arrows), tubular epithelium (white arrows), and tubulointerstitium (white arrowhead) of WT and *cd44–/–* mice. Bar = 50 μm. To optimize viewing of this image, please see the online version of this article at www.kidney-international.org.

Figure 5a, NTS-injected WT mice consistently showed an acquired expression of CD44, both in Bowman space and in the tubulo-interstitial space, in particular in periglomerular areas. Using a combined immunohistochemical and histochemical staining for CD44 and periodic acid–Schiff (PAS), respectively (similar to the staining displayed in Figure 1e and f), we detected that all glomeruli with early and advanced proliferative lesions in Bowman space were positive for CD44 (data not shown). Within the glomerulus, CD44 co-localized with the PEC markers SSeCKS (Figure 5a) and claudin-1 (Figure 5b) but not with the podocyte marker synaptopodin (Figure 5a). Saline-treated WT mice did not reveal a glomerular CD44 staining nor claudin-1 staining in the glomerular tuft (data not shown). As expected, NTS-injected *cd44–/–* mice did not display renal CD44 expression, and fewer SSeCKS and claudin-1 positive lesions were observed (Figure 5a and b). Next, we evaluated whether the CD44-positive PEC population was the primary origin of the proliferating PEC population. To this end, we performed a triple staining for CD44, SSeCKS, and Ki67 (Figure 5c). We found that most (78% ± 7%) of the Ki67-positive PECs were CD44-positive as well.

Although our data suggest that the differences in glomerular cell proliferation between NTS-injected WT and *cd44–/–* mice may be explained by a reduced presence of activated PECs in *cd44–/–* mice, another explanation could be differences in glomerular influx of inflammatory cells. However, counting the number of granulocytes, macrophages, and CD8- and CD4-positive T cells revealed no significant differences between NTS-injected WT and *cd44–/–* mice (Figure 6a–d). A representative result for macrophage staining in WT and *cd44–/–* mice is depicted in Figure 6e. A separate count of the number of macrophages in the periglomerular space revealed a difference between WT and *cd44–/–* mice—the latter displayed fewer macrophages (Figure 6f).

CD44 deficiency reduces proteinuria and glomerular cell proliferation in collapsing FSGS

To validate our findings obtained in experimental crescentic glomerulonephritis, we employed the anti-Thy1.1 model for collapsing FSGS, in WT *Thy1.1* transgenic (tg) mice and *Thy1.1* tg *cd44–/–* mice. Anti-Thy1.1 injection in *Thy1.1* tg mice normally induces proteinuria within 1 hour, and typical

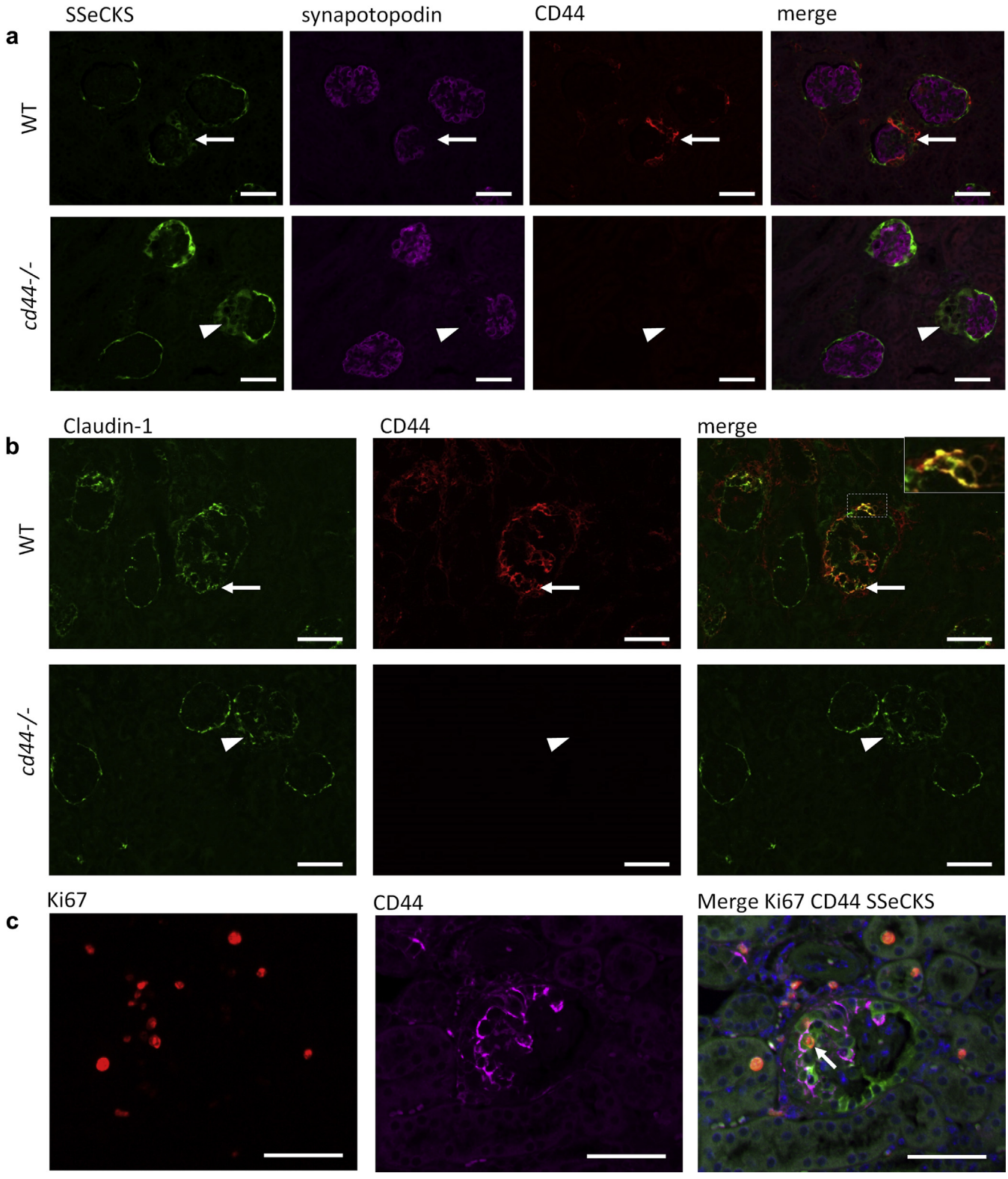

Figure 5 | Fewer parietal epithelial cells (PECs) in crescentic lesions in cluster of differentiation 44–deficient (*cd44–/–*) mice. To detect the presence of PECs in crescentic lesions, immunostaining was performed for the PEC markers SSeCKS (**a**) and claudin-1 (**b**). Wild-type (WT) nephrotoxic serum (NTS)–injected mice showed an acquired expression of CD44 in SSeCKs (arrows, **a**) and claudin-1–positive PECs (arrows and inset, **b**), which was not present in the *cd44–/–* mice (**a**, arrowheads). NTS-injected *cd44–/–* mice showed no acquired CD44 expression and less SSeCKS- and claudin-1–positive lesions (arrowheads, **a** and **b**, respectively). Also, no colocalization was seen between SSeCKS or CD44 and the podocyte marker synaptopodin (**a**). Triple immunofluorescence staining for Ki67, CD44, and SSeCKS (**c**). Nuclei are stained with 4′,6-diamidino-2-phenylindole (blue). Using these three markers, we were able to establish the percentage of Ki67-positive cells present in PECs (SSeCKS positive) and in activated PECs (CD44- and SSeCKS-positive; arrow). Bar = 50 μm. To optimize viewing of this image, please see the online version of this article at www.kidney-international.org.

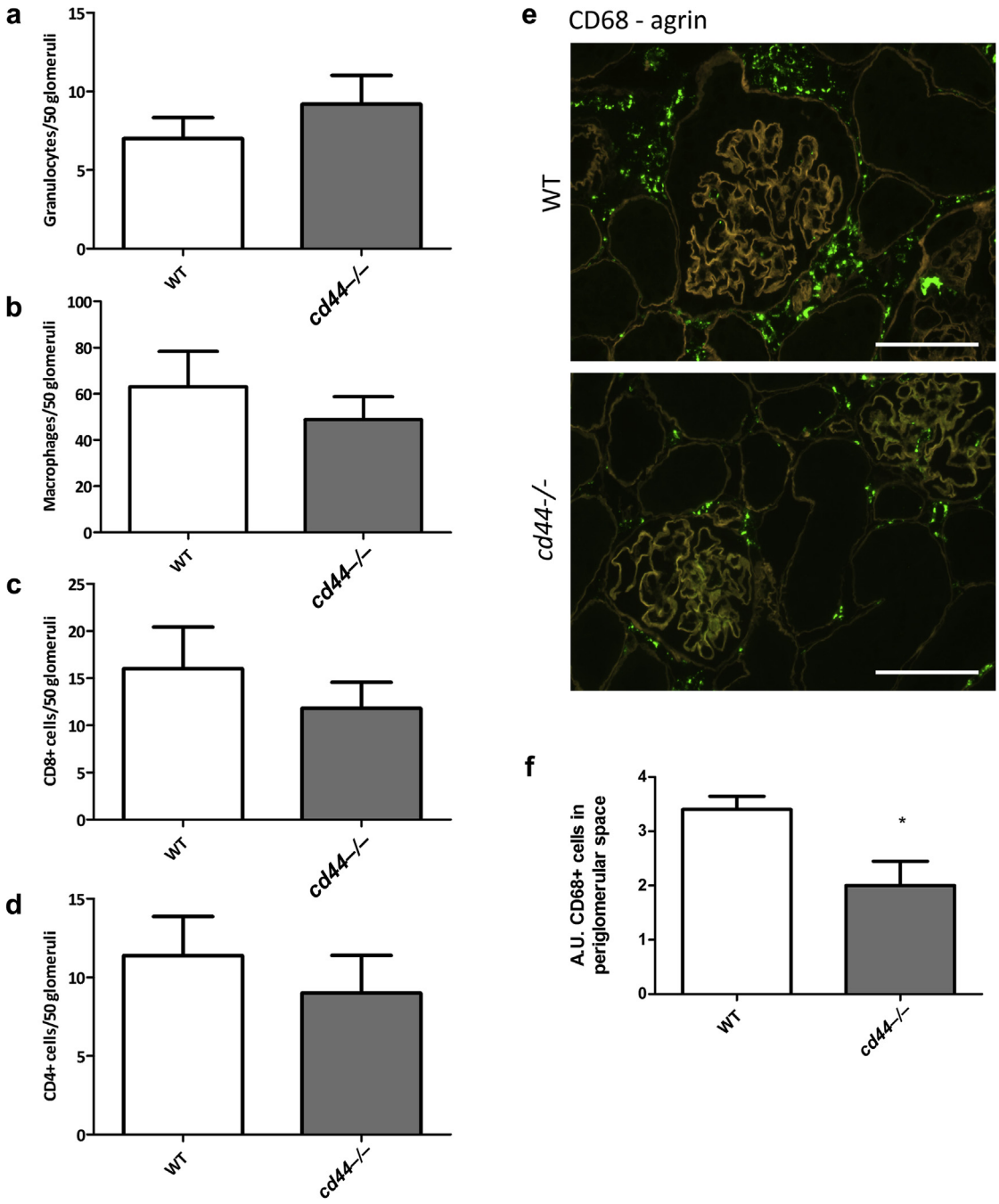

Figure 6 | No differences in the glomerular influx of inflammatory cells. Number of granulocytes, macrophages, and cluster of differentiation (CD)8- and CD4-positive T cells in wild-type (WT) and CD44-deficient (*cd44–/–*) mice (**a–d**). Double staining for CD68 and agrin was performed to analyze the macrophage influx on the renal cryosections of WT and *cd44–/–* mice (**e,f**). Periglomerular macrophage influx was scored semiquantitatively based on CD68-positive staining on a scale of 0 to 5 (**f**). The number of positive cells per 50 glomeruli is represented as mean ± SEM, for WT and *cd44–/–* mice (n = 5). *$P < 0.05$. Bar = 50 μm. A.U., arbitrary unit. To optimize viewing of this image, please see the online version of this article at www.kidney-international.org.

sclerotic lesions develop within 7 days.[4] After 8 days, we analyzed the renal expression of CD44, which revealed that saline-injected *Thy1.1* tg mice displayed no renal CD44 expression (data not shown), whereas anti-Thy1.1 mAb-injected *Thy1.1* tg mice, but not *Thy-1.1* tg *cd44–/–* mice, acquired glomerular, periglomerular, and tubular CD44 expression (Figure 7a, b). We found that, as in the NTS model, 100% of the lesions detected in the PAS staining were positive for CD44 (Figure 7a).

The urinary albumin:creatinine ratio of *Thy1.1* tg *cd44–/–* mice was 2-fold lower, compared with WT *Thy1.1* tg mice (Figure 7c). Renal function did not differ between WT *Thy1.1*

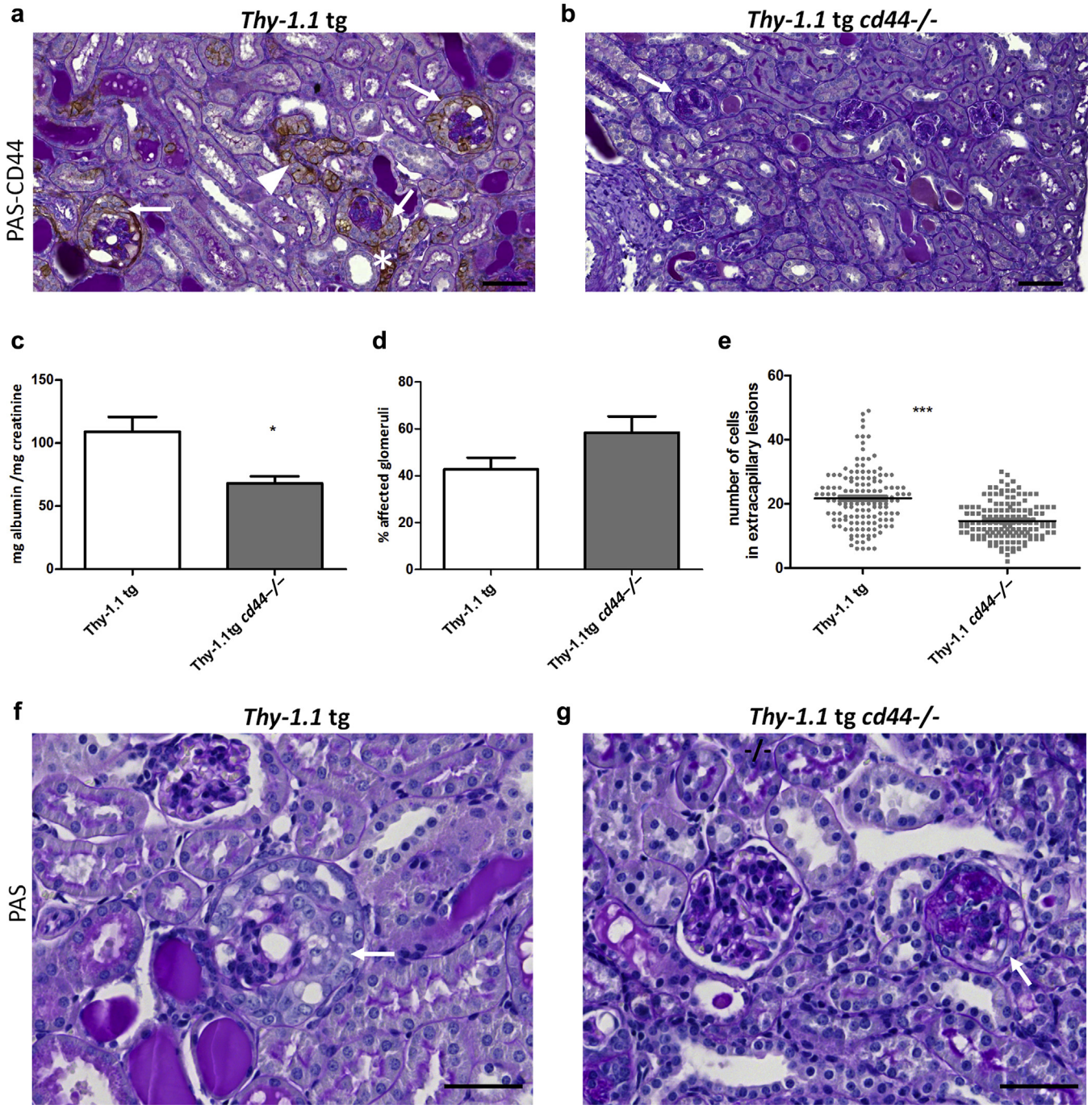

Figure 7 | Cluster of differentiation (CD)44 deficiency reduces proteinuria and the number of cells in extracapillary lesions in the *Thy1.1* transgenic (tg) collapsing focal and segmental glomerulosclerosis model. Immunostaining for CD44 on a periodic acid–Schiff (PAS)–stained section of a *Thy-1.1* tg (**a**) and a *Thy-1.1* tg CD44-deficient (*cd44–/–*) mouse (**b**), respectively. Only in the wild-type (WT) mouse immunostaining was CD44 detected in the epithelial cells of affected glomeruli (arrow), tubuli (arrowhead), and periglomerular areas (asterisks). Proteinuria expressed as mg albumin/mg creatinine ratio in *Thy1.1* tg and *Thy1.1* tg *cd44–/–* mice on day 8 after anti-Thy1.1 mAb injection (**c**). Formation of collapsing lesions in the glomeruli was determined by an analysis of at least 50 glomeruli per mouse and expressed as the percentage of affected glomeruli in *Thy1.1* tg and *Thy1.1* tg *cd44–/–* mice (**d**). Assessment of the number of nuclei in extracapillary lesions in *Thy1.1* tg and *Thy1.1* tg *cd44–/–* mice (**e**). Data are given as mean ± SEM for *Thy1.1* tg (n = 8) and *Thy1.1* tg *cd44–/–* (n = 7) mice. Mann-Whitney U test (2-tailed); $^{*}P < 0.05$; $^{***}P < 0.001$. Representative images of PAS-stained sections of *Thy1.1* tg (**f**) and *Thy1.1* tg *cd44–/–* mice (**g**). Hyperplasia or multilayered accumulation of cells forming (pseudo)-crescents (**f,g**, arrows). Bar = 50 μm. To optimize viewing of this image, please see the online version of this article at www.kidney-international.org.

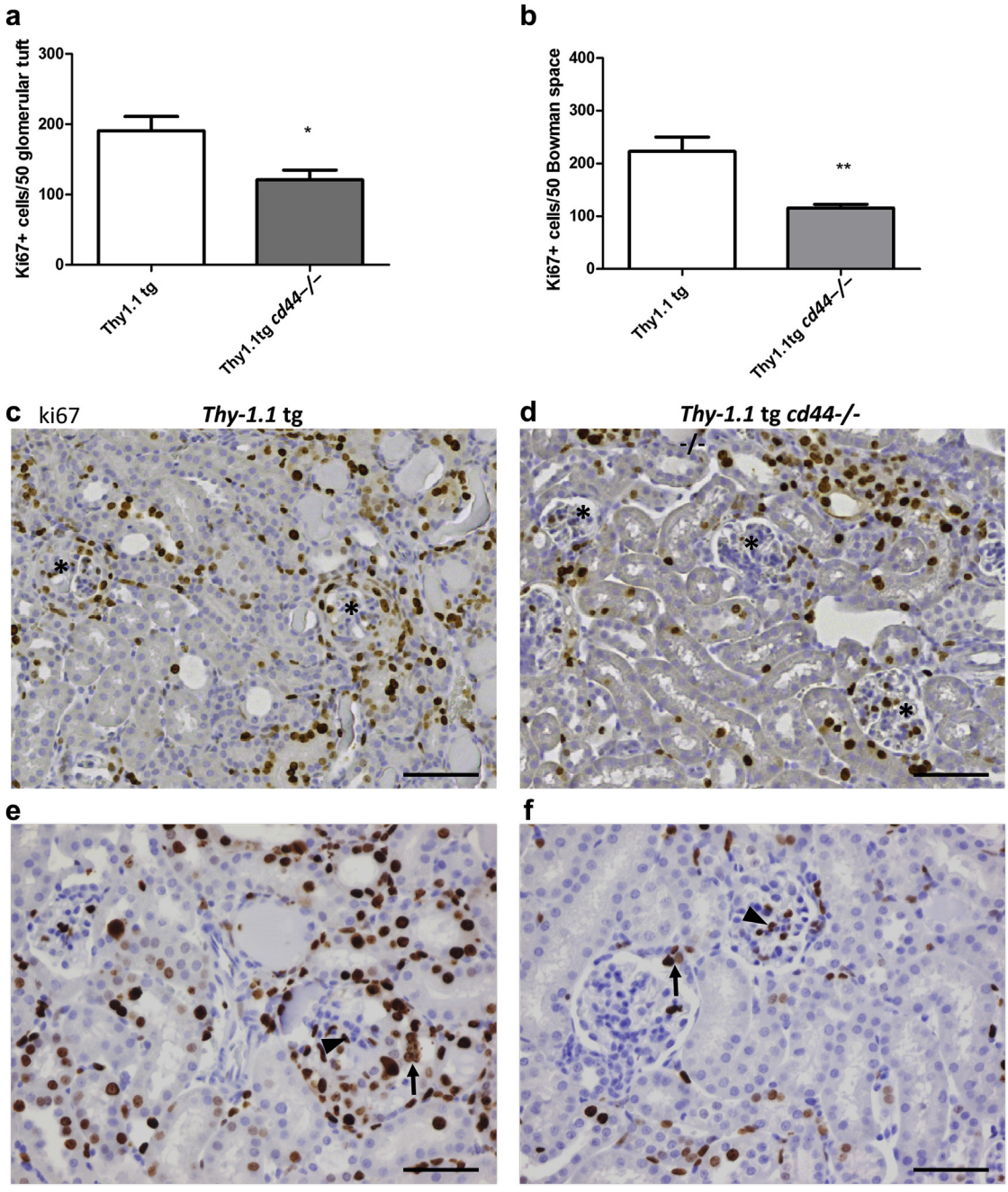

Figure 8| Cluster differentiation (CD)44 deficiency reduces glomerular cell proliferation in the Thy1.1 transgenic (tg) collapsing focal and segmental glomerulosclerosis model. Total numbers of Ki67-positive cells located in the glomerular tuft (**a**) and Bowman space (**b**) were counted per 50 glomeruli of *Thy1.1* transgenic (tg) and *Thy1.1* tg *cd44–/–* mice on 3,3′-diaminobenzidine–stained formalin-fixed paraffin sections. Data are given as mean ± SEM for *Thy1.1* tg (n = 8) and *Thy1.1* tg *cd44–/–* mice (n = 7). Mann-Whitney U test (2-tailed); $*P < 0.05$; $**P < 0.01$. Representative images showing Ki67-positive cells 8 days after anti-Thy1.1 injection in *Thy1.1* tg (**c,e**) and *Thy1.1* tg *cd44–/–* mice (**d,f**). Marked proliferation was detected in the glomeruli (asterisks, **c**,**d**) in both the glomerular tuft (arrowheads, **e,f**) and Bowman space (arrows, **e,f**). Bar = 100 μm (**c**,**d**). Bar = 50 μm (**e**,**f**). To optimize viewing of this image, please see the online version of this article at www.kidney-international.org.

tg and *Thy1.1* tg *cd44–/–* mice, with respective blood urea nitrogen values of 18.5 ± 1.8 mmol/L versus 16.1 ± 2.1 mmol/L.

Despite the differences in albuminuria, analysis of renal histology revealed no significant difference in the percentage of affected glomeruli, in a comparison of anti-Thy1.1-injected WT *Thy1.1* tg and *Thy1.1* tg *cd44–/–* mice (Figure 7d). Both WT *Thy1.1* tg and *Thy1.1* tg *cd44–/–* mice displayed the typical lesions we normally observe in the anti-Thy1.1 model (Figure 7f and g), with collapse of the glomerular tuft and marked hyperplasia in Bowman space. However, quantitative assessment of the number of nuclei within the extracapillary cellular lesions revealed a reduced number of cells in the

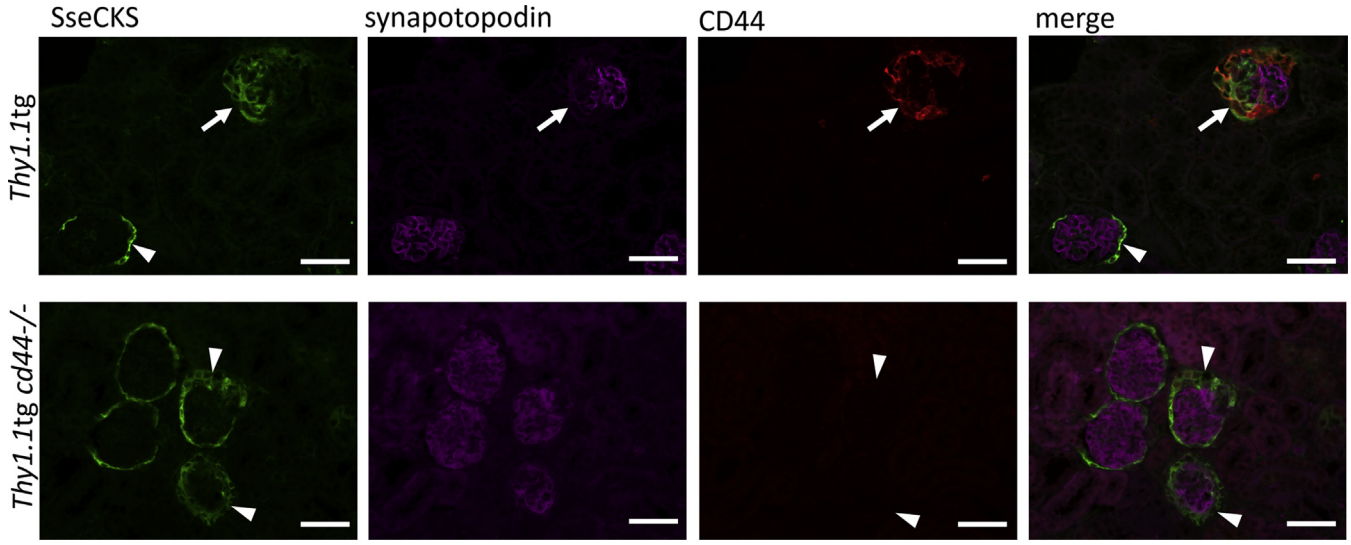

Figure 9 | Fewer parietal epithelial cells (PECs) in collapsing focal and segmental glomerulosclerosis lesions in cluster of differentiation 44–deficient (*cd44–/–*) mice. To detect the presence of PECs in collapsing lesions, immunostaining was performed for the PEC marker SSeCKS. *Thy1.1* transgenic (tg) mice injected with anti-Thy-1.1 mAb showed an acquired expression of CD44 in SSeCKS-positive PECs (arrows). In contrast, *Thy1.1* tg *cd44–/–* mice did not show acquired CD44 expression in SSeCKS-positive lesions (arrowheads). No colocalization was seen between SSeCKS or CD44 with the podocyte marker synaptopodin. Bar = 50 μm. To optimize viewing of this image, please see the online version of this article at www.kidney-international.org.

lesion of the *Thy-1.1*tg *cd44–/–* mice, compared with the WT *Thy1.1* tg mice (Figure 7e).

In accordance with the results just described, the number of Ki67-positive cells in Bowman space was significantly lower in *Thy1.1* tg *cd44–/–* mice compared with WT *Thy1.1* tg mice. A similar difference, to a lesser extent, was seen for the Ki67-positive cells in the glomerular tuft (Figure 8a–f). As in the NTS model, the extracapillary proliferative lesions were positive for the PEC marker SSeCKS, which was less pronounced in *Thy1.1* tg *cd44–/–* mice (Figure 9). As in the NTS model, triple staining for CD44, SSeCKS, and Ki67 revealed that in the anti-Thy-1.1 model, the vast majority (92% ± 4%) of the Ki67-positive PECs were CD44-positive as well.

CD44 deficiency reduces growth of PECs in culture

To examine the effects of CD44 deficiency on the behavior of PECs, we performed a glomerular outgrowth assay as described elsewhere.[28] In this assay, we assessed the glomerular epithelial outgrowth after culturing single isolated capsulated mouse glomeruli. Capsulated glomeruli were isolated from the *cd44–/–* and WT mice and cultured for 6 days, after which the percentage of glomeruli with an outgrowth and the surface area of the outgrowth was assessed for more than 500 glomeruli. The percentage of glomeruli that formed an outgrowth was reduced in the CD44-deficient glomeruli (Figure 10c–e). Also, the surface area of the outgrowths was smaller in this group, indicating that CD44 is directly involved in glomerular epithelial cell growth (Figure 10f). In the WT outgrowths, the cells were CD44-positive, unlike those from CD44-deficient glomeruli (Figure 10g and h). By analyzing outgrowths at day 6, we were able to focus on the growth of the fast-growing PECs, rather than podocytes that need at least 7 to 14 days to form an outgrowth.[29] This was further supported by the finding that glomeruli without a capsule (n = 24) did not form outgrowths at day 6 (Figure 10i). In addition, immunostaining for PEC (SSeCKS, claudin-1) and podocyte (synaptopodin) markers revealed homogenous staining of the outgrowth for SSeCKS (Figure 10j–l) and claudin-1 but not for synaptopodin (Supplementary Figure S2).

Collagen I and IV drive PEC migration *in vitro* in a CD44-dependent manner

Matrix deposition is a key feature of lesion or crescent formation. Collagen I normally is not expressed in the glomerulus, but it is observed in various glomerulopathies.[30,31] In both models, we observed increased cortical collagen I alpha 1 and IV mRNA expression, which was about 2-fold less in CD44-deficient mice (data not shown). In addition, PECs produce matrix within the sclerotic lesions and crescents. In earlier studies, we and others showed that the matrix in the lesions resembled the matrix of Bowman capsule, containing collagen IV alpha 1, 2, and 6. Therefore, we postulated that collagen I and IV may be involved in PEC migration. To test this *in vitro*, we employed human PECs that expressed CD24, CD133, and CD44 (Supplementary Figure S3) in a haptotaxis assay. Notably, established hPEC clones always express CD44, which may suggest that these cultured hPECs have an activated phenotype. The haptotaxis assay revealed maximal migration of hPECs towards collagen I and collagen IV at a coating concentration of 50 μg/ml (Figure 10a and b). Given that the PECs expressed CD44, we evaluated the effect of neutralizing

CD44 with an anti-CD44 antibody, which revealed a significantly decreased migration of hPECs, whereas an isotype control antibody had no effect (Figure 11a and b). As most of the Ki67-positive PECs *in vivo* were CD44-positive, we postulated that CD44 is important for cell activity and proliferation. To test this *in vitro*, we performed a cell metabolic activity assay (MTT assay) and evaluated the effect of neutralizing CD44 with anti-CD44. However, neutralizing CD44 did not produce a significant effect ($P = 0.07$) on cell activity (Figure 11c).

CD44 deficiency does not affect Erk1/2, YAP, and STAT3 signaling in PECs during experimental crescentic glomerulonephritis and collapsing focal segmental glomerulosclerosis

In the previous section, we showed *in vitro* that collagen I and IV drive PEC movement in a CD44-dependent manner, whereas CD44 neutralization tended to affect PEC proliferation as well ($P = 0.07$). To gain further mechanistic insight into the role of CD44 *in vivo*, we analyzed different signaling pathways in WT and *cd44–/–* kidneys of the NTS and anti-Thy1.1 model. Although numerous downstream signaling pathways and factors that link to CD44 have been described, we choose to limit our analysis to 3 candidates: phospho-Erk1/2 (p-Erk1/2), Yes-associated protein (YAP), the effector of the Hippo pathway, as well as phospho-signal transducer and activator of transcription 3 (p-STAT3). Notably, the aforementioned factors are part of signaling pathways that all have been linked to CD44 and regulation of cell migration and/or proliferation.[32–34] We observed in both the NTS and anti-Thy1.1 model an increased immunostaining for p-Erk1/2 (Supplementary Figure S4A and B) and YAP in the CD44-positive PECs (Supplementary Figure S5A and B). Notably, the overall staining for p-Erk1/2 and YAP appeared less pronounced in CD44-deficient mice compared with WT mice. However, also in CD44-deficient mice, we observed an increased immunostaining of p-Erk1/2 and YAP in PECs in glomerular lesions, which suggests that the expression of these signaling molecules is not (solely) dependent on CD44. Finally, for both the NTS and anti-Thy1.1 model, we did not observe expression of p-STAT3 expression in CD44-positive PECs (Supplementary Figure S5C), which suggests that CD44 and pSTAT3 signaling are not linked to proliferating PECs.

DISCUSSION

Normally, CD44 is not expressed in the glomerulus, and studies in animals and humans have shown that CD44 can be considered to be a specific marker of activated PECs that invade the glomerular tuft during scarring glomerular diseases.[4,10,11,19] Our main research question was whether acquired glomerular CD44 expression can be considered a contributing factor in scarring glomerular diseases. Our results reveal that CD44 deficiency changes the outcome of experimental crescentic glomerulonephritis and collapsing FSGS. In both models, we observed that CD44 deficiency results in less glomerular cell proliferation and reduced albuminuria. These findings are in line with those of a recent study performed independently in a different podocyte injury mouse model. That study also found that CD44-deficient mice had a better outcome, with reduced albuminuria and PEC proliferation.[35] For crescentic glomerulonephritis, the number of histologically affected glomeruli was significantly reduced in the absence of CD44. Even though the number of histologically affected glomeruli was not different in the collapsing FSGS model, a striking difference was found in the number of cells within the extracapillary proliferative lesions. Although, we considered both models to be valid for studying the role of CD44 in scarring glomerular disease,[4] they are different in regard to pathogenesis, which could explain the difference seen in histologic outcome relating to CD44 deficiency.

In experimental crescentic glomerulonephritis, fixation of injected antibody to the GBM leads to complement activation, infiltration of polymorphonuclear neutrophils and macrophages, and crescent formation.[36–39] The cellular crescents formed during crescentic glomerulonephritis are mainly comprised of activated PECs,[12] macrophages,[40] and podocytes.[41] Notably, CD44 is expressed by both activated PECs and macrophages under pathologic conditions, and macrophage depletion has been shown to be beneficial in crescentic glomerulonephritis.[42] Macrophages produce cytokines and pro-fibrotic factors, such as tumor necrosis factor–α, transforming growth factor–β, platelet-derived growth factor, interleukin-1, and fibroblast growth factor–2, and thereby contribute to the formation of crescents.[43] However, our data show that CD44 deficiency in crescentic glomerulonephritis leads to a reduced presence of PECs in Bowman space, whereas the number of glomerular macrophages was not significantly affected. These observations indicate a link among CD44-expressing activated PECs, the formation of crescents, and the development of albuminuria. However, we use a conventional *cd44* knock-out mouse model, so alternative explanations for the reduction in albuminuria due to the global CD44 deficiency are possible. We cannot exclude the possibility that the reduced pathology and PEC hyperplasia within the glomerulus in *cd44–/–* deficient mice may be driven (in part) by other cell types and processes not evaluated in this study. Furthermore, our aim was to analyze the effect of CD44 on crescent formation, so we did not evaluate earlier time points, which could have revealed that CD44 deficiency resulted in less glomerular influx of polymorphonuclear neutrophils, and thereby less glomerular damage and albuminuria.[39,44,45] On the other hand, the *in vitro* studies performed on WT and CD44-deficient glomeruli did reveal a direct relationship between CD44 and growth of PECs, as the formation of outgrowths, consisting of PECs, was reduced in cd44–/– glomeruli, compared with WT glomeruli.

The anti-Thy1.1 model for collapsing FSGS is induced by hitting podocytes with anti-Thy1.1 antibody, which results in podocyte injury and activation of PECs. The subsequent formation of adhesions between the glomerular capillary tuft

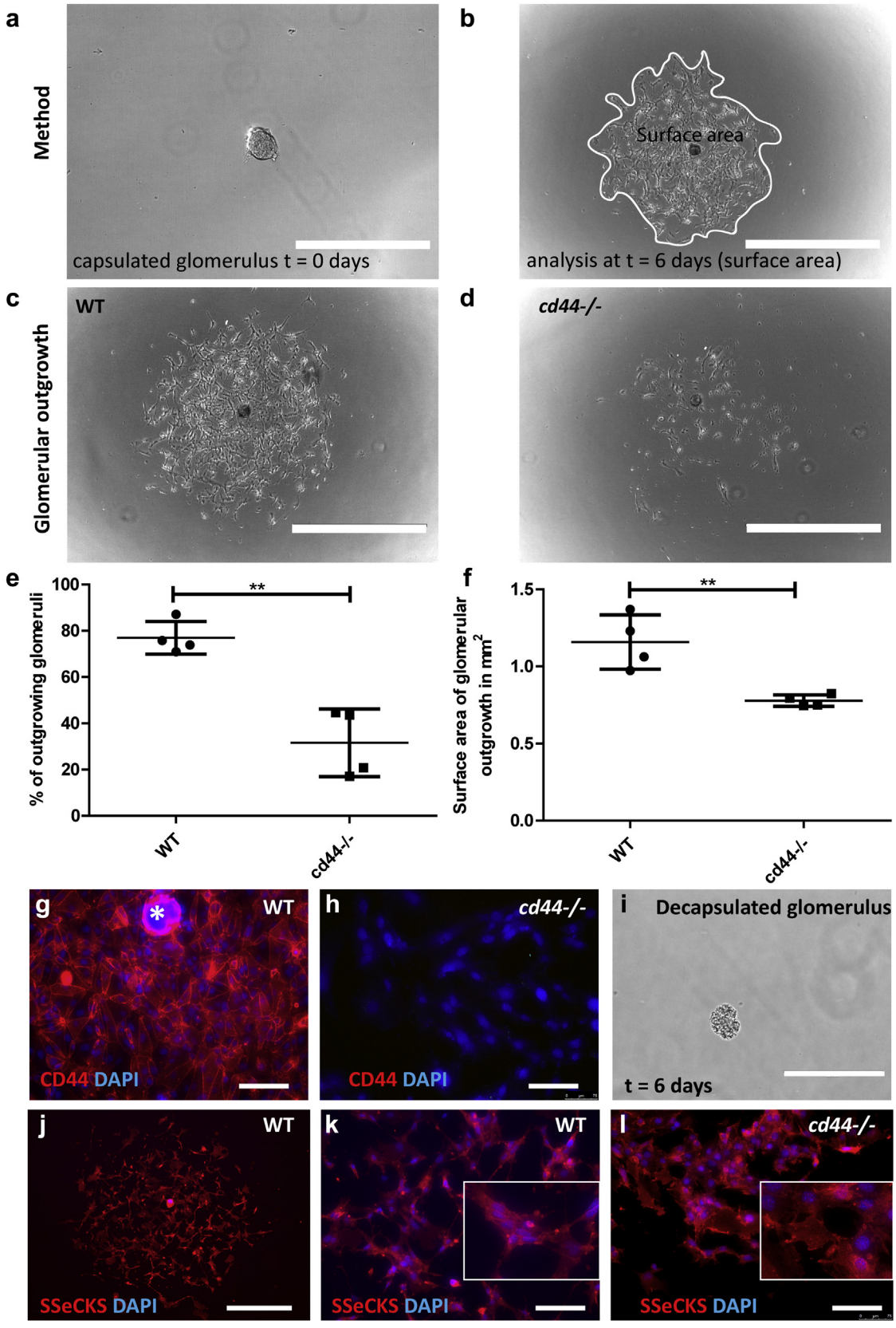

Figure 10 | Cluster of differentiation (CD)44 deficiency reduces growth of parietal epithelial cells (PECs) in culture. Capsulated glomeruli were isolated from CD44-deficient (*cd44–/–*) mice and wild-type (WT) control mice. Single capsulated glomeruli were isolated in a 24-well plate (**a**) and cultured for 6 days. Cellular outgrowths were analyzed at day 6. Cellular outgrowth was impaired by CD44 KO (**b**,**c**,**d**). (Phase contrast image [**a–d**]). The percentage of glomeruli forming outgrowths was significantly lower for CD44-deficient mice (**e**). The surface (continued)

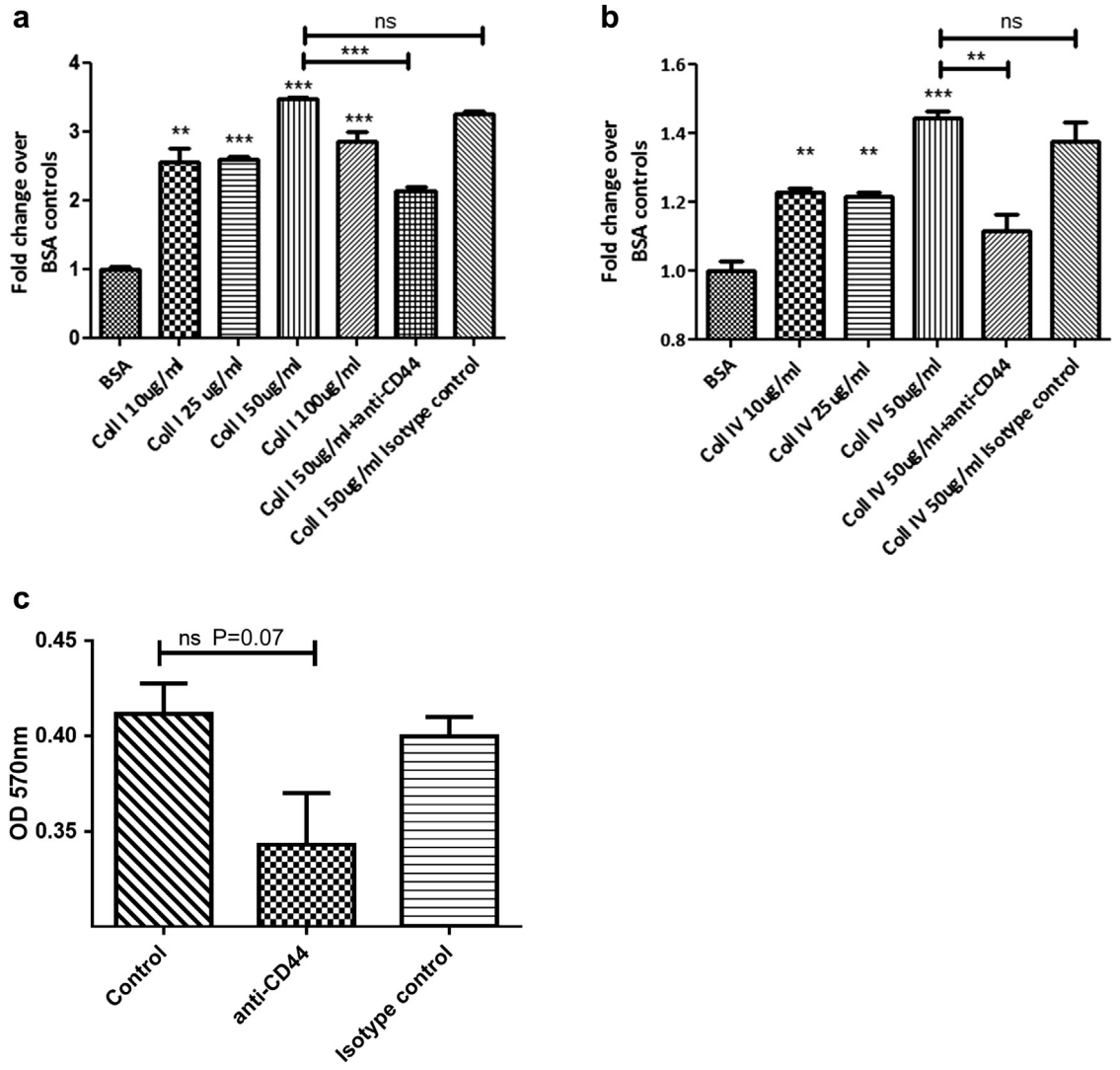

Figure 11 | Cluster of differentiation (CD)44 inhibition reduced collagen I– and IV– induced migration. Haptotactic migration under the influence of various concentrations of collagen I (**a**), collagen IV (**b**), and CD44-neutralizing antibodies. CD133+/CD24+/CD44+ cells were allowed to migrate under the influence of collagen I or collagen IV coatings to the underside of the transwell insert (10–100 ug/ml). For neutralization, cells were pre-incubated for 30 minutes with anti-CD44 antibodies or isotype controls. Fold change was calculated over bovine serum albumin (BSA)–coated controls. Data are given as mean ± SEM (n = 3). ***$P < 0.001$; **$P < 0.01$, for BSA versus collagen I or collagen IV. The cell activity of CD133+/CD24+/CD44+ cells was measured using an MTT (3-[4,5-dimethylthiazol-2-yl]-2,5-diphenyltetrazolium bromide) tetrazolium assay. The cells were nontreated or pre-incubated for 24 hours with anti-CD44 antibodies or isotype control (**c**). coll, collagen; ns, nonsignificant; OD, optical density.

and Bowman capsule provides an entry site for activated PECs.[10,19] Activated PECs contribute to deposition of extracellular matrix material, which ultimately results in segmental and global glomerulosclerosis. We observed that the number of glomerular proliferating cells is reduced in the absence of CD44, which most likely can be explained by a reduction in proliferating PECs, because the anti-Thy1.1 model is not characterized by massive glomerular influx of immune cells. Despite a reduced number of proliferating glomerular cells and reduced albuminuria, the absence of CD44 did not result

Figure 10 | (continued) areas of the outgrowths of the *cd44–/–* glomeruli were significantly smaller compared with the areas measured from the WT mice (**f**). Data are given as mean ± SD (n = 4). **$P < 0.01$. The outgrowths of the WT glomeruli showed a strong expression of CD44 (**g**). CD44 staining also was observed surrounding the glomerulus (**g**, asterisk). CD44 immunostaining was not detected in cells from the *cd44–/–* mice (**h**). Decapsulated glomeruli (n = 24) did not form outgrowths at day 6 (**i**). The outgrowths showed a homogenous immunostaining for the PEC marker SSeCKS in both the WT (**j,k**) and *cd44–/–* mice (**l**). Bars = 400 μm (**a,j**); 1000 μm (**b–d**); 200 μm (**i**); and 100 μm (**g,h,k,l**). Inserts: x2 zoom (**k,l**). DAPI, 4′,6-diamidino-2-phenylindole. To optimize viewing of this image, please see the online version of this article at www.kidney-international.org.

in less histologically affected glomeruli at the selected time point. One possible explanation could be that we have evaluated the kidneys too early, as persistently higher proteinuria may lead to further progression of the glomerular injury and induce additional lesions.[46] We have no direct explanation for the fact that the degree of albuminuria is not related to overall histology in collapsing FSGS. Apparently, the number of glomerular proliferating cells is a more sensitive parameter that can be related to albuminuria rather than to histology in the 2 tested models of glomerular scarring, as was suggested recently for proliferating cells in the urine of FSGS patients.[47]

The number of glomerular proliferating cells also was related to cortical collagen I expression in both models. Notably, collagen IV is the type of collagen expressed in both normal and diseased glomeruli (sclerosis), whereas collagen I is normally not expressed in the glomerulus, but several studies have shown glomerular collagen I expression in various glomerulopathies.[48–50] We found an increased collagen I expression in both models tested. We reasoned that the extracellular matrix delivers signals to activated PECs, so we tested the migratory capacity of CD44 expressing human PECs towards collagen I and collagen IV *in vitro* and indeed found migration of PECs in a CD44-dependent manner, whereas neutralization of CD44 tended ($P = 0.07$) to reduce PEC cell activity/proliferation *in vitro* as well. CD44 is known to be involved in many cellular processes, including cell migration and proliferation.[51] In addition, many downstream signaling pathways and factors have been linked to CD44 and cell migration/proliferation, such as phospho-Erk1/2 (p-Erk1/2), Yes-associated protein (YAP), the effector of the Hippo pathway, and phospho-signal transducer and activator of transcription 3 (p-STAT3). Although p-Erk1/2 and YAP were upregulated in the hyperplastic lesions, analysis of these signaling molecules did not reveal a clear difference between WT and *cd44–/–* mice in our NTS and anti-Thy1.1 model, which suggests that along with CD44-mediated signaling, other pathways are operative. A recent study found that Erk1/2 induce CD44 expression in PECs, leading to a pro-sclerotic and migratory PEC phenotype.[35] Another complicating factor is that CD44 has many splice variants, which each have specific binding partners, thereby linking to various signaling pathways. Elucidation of the exact molecular mechanisms underlying proliferation of CD44-positive PECS during experimental crescentic glomerulonephritis and collapsing FSGS, as well as the CD44-mediated haptotactic response of human PECs toward collagen I and collagen IV requires substantial additional research.

Acquired glomerular CD44 expression by activated PECs is required for the pathogenesis of experimental crescentic glomerulonephritis and collapsing FSGS.

METHODS

Animals and animal experiments

Wild type (WT), CD44-deficient (*cd44–/–*), Thy1.1 transgenic (*Thy1.1* tg), and *cd44–/– Thy1.1* tg mice were all on a C57Bl/6 background. The genotype and phenotype of these mice have been described previously, whereas the *cd44–/– Thy1.1* tg mice were obtained by cross-breeding *cd44–/–* mice with *Thy1.1* tg mice in the current study.[44,52] All animal experiments were approved by the Animal Ethics Committee of the Radboud University Nijmegen and conducted in accordance with the European Communities Council Directive (86/609/EEC).

Crescentic glomerulonephritis was induced as described previously.[53] Briefly, 7-week-old WT and *cd44–/–* mice were injected i.p. with 4 mg nephrotoxic serum (NTS) supplemented with 80 μg CpG Oligo (tebu-bio, Heerhugowaard, The Netherlands).

Urine was collected at day 13 in metabolic cages, for 18 hours. Mice were sacrificed at day 14, and kidneys and blood were collected.

Collapsing FSGS was induced as described previously.[52] Briefly, 7-week-old *Thy1.1* tg and *Thy1.1* tg *cd44–/–* mice were injected i.v. with 1 mg anti-Thy1.1 monoclonal antibody. Urine was collected at day 7 in metabolic cages, for 18 hours. Mice were sacrificed at day 8, and kidneys and blood were collected.

Albumin in urine was measured by radial immunodiffusion (Mancini), and urinary creatinine and plasma ureum concentrations were determined in the clinical diagnostic facility of Radboudumc.

Renal histology

Renal paraffin sections (4 μm) were deparaffinized, dehydrated, and stained with PAS stain. Fifty glomeruli per mouse were evaluated for hypertrophy, hyperplasia, sclerosis, adhesions, or hyalinosis, which were expressed as a percentage of affected glomeruli. Evaluation of histology was performed on blinded sections by 2 nephropathologists.

Proliferating cells were immunostained for the Ki67 proliferation marker, as described later (immunohistochemistry staining), and positive nuclei were counted in 50 glomeruli per mouse on blinded sections. To assess CD44 expression in relation to the histology, a CD44 immunostaining was combined with a PAS staining. Glomerular histology and the presence of CD44 was evaluated in all glomeruli present in the section.

Immunohistochemistry staining

Immunohistochemistry was performed on 4-μm paraffin. CD44 immunostainings were combined with a PAS staining. Sections were blocked with Avidin/Biotin Blocking Kit (Vector Laboratories, Burlingame, CA) and 3% H_2O_2. The sections were subjected to microwave antigen retrieval in citrate buffer with pH 6, followed by incubation with the primary (Table 1) and secondary antibodies. For secondary antibodies, we used biotinylated goat anti-rabbit (Ki67) or goat anti-rat (CD44) (Vector Laboratories). Detection was carried out with Vectastain ABC Kit (Vector Laboratories), with peroxidase used as a label, and 3,3′-diaminobenzidine used as a substrate. Subsequent to the CD44 immunostaining, PAS staining was performed.

Immunofluorescence staining

Immunofluorescence staining was performed on renal cryosections (2 μm) or formalin-fixed paraffin sections (4 μm) as described previously.[39] The primary antibodies used are listed in Table 1. Appropriate Alexa conjugated antibodies (Invitrogen Life Technologies, Breda, The Netherlands) were used for detection. Stained sections were post-fixed with 1% paraformaldehyde–phosphate buffer saline and embedded in VectaShield mounting medium H-1000 (Brunschwig Chemie, Amsterdam, The Netherlands). Staining intensities were scored semi-quantitatively for 50 glomeruli per mouse, by 2 researchers, using a fluorescent microscope (Leica Microsystems, GmbH, Germany). The number of granulocytes,

Table 1 | Primary antibodies used

Antibody	Manufacturer
Anti-agrin (MI91)	Laboratory collection[54]
Anti-C3c (FITC labeled)	Nordic, Tilburg, The Netherlands
Anti-CD4	BD Biosciences, Alphen aan de Rijn, The Netherlands
Anti-CD8a	BD Biosciences, Alphen aan de Rijn, The Netherlands
Anti-CD24	Santa Cruz Biotechnology, Santa Cruz, CA
Anti-CD44	BD Biosciences, Alphen aan de Rijn, The Netherlands
Anti-CD68	Serotec, Oxford, United Kingdom
Anti-CD133	Miltenyi Biotec GmbH, Bergisch Gladbach, Germany
Anti-claudin1	Abcam, Cambridge, United Kingdom
Anti-fibrinogen (FITC labeled)	Nordic, Tilburg, The Netherlands
Anti-Ly-6G (FITC labeled)	BD Biosciences, Alphen aan de Rijn, The Netherlands
Anti-SSeCKS	Origene, Rockville, MD
Anti-synaptopodin	Santa Cruz Biotechnology, Santa Cruz, CA
Anti-Ki67 (clone sp6)	Thermo Scientific, Breda, The Netherlands
Anti-phospho-STAT3	Cell Signaling Technology, Leiden, The Netherlands
Anti-phospho-Erk1/2	Cell Signaling Technology, Leiden, The Netherlands
Anti-YAP	Cell Signaling Technology, Leiden, The Netherlands

CD, cluster of differentiation; FITC, fluorescein isothiocyanate.

macrophages, CD4- and CD8a-positive T cells was counted in 50 glomeruli per mouse.

Triple immunofluorescence staining for Ki67, CD44, and SSeCKS on paraffin sections needed a different protocol, as 2 of the primary antibodies (anti-Ki67 and anti-SSeCKS) were rabbit polyclonal antibodies. To circumvent cross-reaction between both markers, we stained Ki67 using the Alexa Fluor 488 Tyramide SuperBoost Kit, (ThermoFisher Scientific, Waltham, MA). After the tyramide-based fluorescence staining, we performed another heat-induced antigen retrieval in citrate buffer with pH 6, for 15 minutes, to remove the bound antibodies. Subsequently, normal immunofluorescence staining was performed for CD44 and SSeCKS. All Ki67- and SSeCKS-positive cells were evaluated to determine whether they also expressed CD44.

Cell culture and flow cytometry

Human PECs (hPECs), in particular CD24 and CD133 double positive cells, were isolated and cultured essentially as described previously.[9] Briefly, glomeruli were isolated from healthy kidney tissue using gradual sieving. Glomeruli were seeded in endothelial cell growth medium EGM-2 MV (Lonza, Breda, The Netherlands), with 20% fetal bovine serum. Cellular outgrowth was harvested and re-seeded. Isolated clones obtained by limiting dilutions were characterized for expression of CD24, CD133, and CD44 using the antibodies listed in Table 1. Immunofluorescence was analyzed on a FC500 Flow Cytometer (Beckman Coulter, Woerden, the Netherlands). One of the isolated clones (3011) was used for *in vitro* experiments.

Glomerular outgrowth assay

Untreated, healthy WT mice (n = 4) and *cd44–/–* (n = 4) mice were sacrificed. Both male and female mice were used. Kidneys were isolated and minced, using 2 scalpels, and then pressed through a 300-μm sieve. The kidney homogenate then was rinsed through a 75-μm sieve and subsequently a 53-μm sieve, using Hanks' Balanced Salt Solution (HBSS) (ThermoFisher Scientific). The kidney structures (glomeruli and tubuli) present on both sieves were collected in Dulbecco's Modified Eagle's Medium (ThermoFisher Scientific, Waltham, MA), supplemented with 20% fetal calf serum (FCS), and transferred into Ultra-Low Attachment Microplates (Corning Costart, Fisher Scientific, Landsmeer, the Netherlands). Single capsulated and decapsulated glomeruli were collected with a pipette under an inverted light microscope and transferred into 24-well plates. Glomeruli were cultured for 6 days at 37° C, 5% CO_2, in endothelial basal medium (EBM #CC-3121, Lonza,) supplemented with EGM-MV Single Quots kit (Lonza), and an additional 5% fetal bovine serum (Lonza) and 1% Pen/Strep. After 6 days, microscopic images were made using light microscopy (EVOS fl microscope, ThermoFisher Scientific), and the percentage of outgrowing glomeruli was determined. In addition, the surface area in mm^2 of glomerular outgrowth was assessed using ImageJ. A total of 523 single glomeruli (248 from WT and 275 from *cd44–/–* mice) were isolated and evaluated. In addition, the outgrowth assay was performed on 24 decapsulated glomeruli. (12 WT and 12 *cd44–/–* glomeruli).

To characterize the outgrowing cells, immunofluorescence staining was performed on outgrowing glomeruli at t = 6 days. For this process, the medium was carefully removed, and glomeruli were washed twice with phosphate buffer saline and fixated for 10 minutes at room temperature using 2% paraformaldehyde + 4% sucrose in phosphate buffer saline, after which cells were washed twice. The cells were stained with primary antibody for SSeCKS, CD44, claudin-1, and synaptopodin and subsequently stained with the secondary antibodies—anti rabbit IgG (H+L) Alexa 568 (ThermoFisher Scientific), anti goat IgG (H+L) Alexa 568, or anti rat IgG (H+L) Alexa 647 (ThermoFisher Scientific). For mounting, DAPI-Fluoromount G (Southern Biotech, Birmingham, AL) was used.

In vitro migration and cell viability assay

Migration of hPECs was studied in transwell cell culture inserts with an 8-μm pore size (Thermo Scientific, Breda, The Netherlands). Inserts were coated at the bottom with indicated concentrations of collagen I, collagen IV, or 2% bovine serum albumin (all Sigma-Aldrich Chemie, Nürnberg, Germany). Serum (EGM-2 MV [Lonza] 0.5% FCS)-starved hPECs were seeded (10^5 cells) in the upper chambers. Where indicated, cells were pre-incubated with anti-CD44 antibody or isotype control. Medium containing 0.5% FCS was added into the lower chambers. After 5 hours, at 37 °C, migrated cells at the bottom side of the inserts were quantified with 0.2% crystal violet. Dye was extracted using 10% glacial acetic acid, and the optical density was measured at 590 nm.

Cell metabolic activity was measured using the MTT assay. Cells grown in EGM-2 MV medium (Lonza), with 20% FCS, were incubated with the CD44 neutralizing antibody or an isotype control antibody for 24 hours prior to the MTT assay.

Cells were incubated in the presence of MTT reagent containing tetrazolium MTT (3-(4, 5-dimethylthiazolyl-2)-2, 5-diphenyltetrazolium bromide (Sigma-Aldrich, St Louis, MO) for 2 to 4 hours, until purple precipitate was visible. The dye was extracted using a detergent reagent, and the optical density was measured at 570 nm.

Statistical Analysis

Results are expressed as mean, ±SEM or ±SD. Groups were compared using a paired *t*-test or Mann-Whitney U test. *P* values of <0.05 were considered statistically significant.

DISCLOSURE

All the authors declared no competing interests.

ACKNOWLEDGMENTS

This study was supported by the Dutch Kidney Foundation (grants C07.2245 and 14A3D10), the Deutsche Forschungsgemeinschaft (DFG; grants BO 3755/2-1, SFB/TRR57 P17 and OS 196/2-1) and The Netherlands Organization for Scientific Research (NWO VIDI: 016.156.363).

SUPPLEMENTARY MATERIAL

Figure S1. Histology of wild type (WT)and cluster of differentiation 44–deficient (*cd44 –/–*) mice. Representative images of periodic acid–Schiff (PAS)–stained sections of nontreated WT control (**A**) and *cd44–/–* mice (**B**). Both the WT and cd44–/– mice showed a normal histology. Bar = 50 μm.

Figure S2. Parietal epithelial cells (PECs) form glomerular outgrowths. Immunostaining for the tight junction molecule claudin-1 (PECs) and the podocyte-specific cytoskeletal protein synaptopodin showed marked immunostaining for claudin-1 within the cell junctions in the glomerular outgrowths. Claudin-1–positive cell junctions were seen in more confluent outgrowths that were obtained with glomeruli from wild type mice. Synaptopodin staining was restricted to the podocytes of the glomerulus (arrow). Outgrowing cells were negative. Bar = 100 μm. DAPI, 4′,6-diamidino-2-phenylindole.

Figure S3. Isolation of human primary parietal epithelial cells (hPECs). Human parietal epithelial cells (hPECs) from glomerular outgrowths were characterized by flow cytometry for cluster of differentiation (CD)24 and CD133. The gated ("target cells") were also positive for CD44 as well as claudin-1 (data not shown).

Figure S4. Cluster of differentiation (CD)44 deficiency does not affect Erk1/2, Yes-associated protein (YAP), or STAT3 signaling in parietal epithelial cells (PECs) during experimental crescentic glomerulonephritis and collapsing focal segmental glomerulosclerosis. Phospho-Erk and CD44 double immunostaining on wild-type (WT) and CD44-deficient (*cd44–/–*) kidney sections treated with nephrotoxic serum. p-ERK was detected in tubular structures and glomeruli. In CD44-negative glomeruli, the PECs were negative or showed a weak staining for p-Erk. A strong increase in expression was detected in CD44-positive PECs (WT, arrows). In *cd44–/–* mice, a lower number of glomeruli showed immunostaining for p-Erk. However, in some glomeruli, clear staining was seen in PECs in lesions or on Bowman capsule (*cd44–/–*, arrow; **A**). The same staining was performed on kidneys sections of anti-Thy-1.1 injected *Thy-1.1* transgenic (tg) and *Thy-1.1* tg *cd44–/–* mice. Strong staining for p-Erk was detected in the CD44-positive PECs in glomerular lesions (*Thy-1.1* tg, arrow). In *Thy-1.1* tg cd44–/– mice, fewer glomeruli showed immunostaining for p-Erk. However, in these mice p-Erk also could be detected in some glomeruli in PECs within lesions (*Thy-1.1* tg cd44–/–, arrow; **B**). Bar = 50 μm.

Figure S5. Cluster of differentiation (CD)44 deficiency does not affect Yes-associated protein (YAP) signaling in parietal epithelial cells (PECs) during experimental crescentic glomerulonephritis and collapsing focal segmental glomerulosclerosis. YAP and CD44 double immunostaining on wild type (WT) and CD44-deficient (*cd44–/–*) kidney sections treated with nephrotoxic serum (NTS). YAP was detected in tubular structures and glomeruli. In CD44- negative glomeruli, the PECs were negative or showed a weak staining for YAP. A strong increase in expression was detected in CD44-positive PECs (WT, arrows). In *cd44–/–* mice, fewer glomeruli showed immunostaining for YAP in PECs. However, as for p-Erk, in some glomeruli, clear staining still was seen in PECs (*cd44–/–*, arrow; **A**). The same staining was performed on kidneys sections of anti-Thy-1.1 injected *Thy-1.1* transgenic (tg) and *Thy-1.1* tg *cd44–/–* mice. An overall strong increase in immunostaining of both tubuli and glomeruli could be noted, and marked staining for YAP was detected in the CD44-positive PECs in glomerular lesions (*Thy-1.1* tg; arrow). In *Thy-1.1* tg *cd44–/–* mice, less YAP immunostaining was detected in tubular and glomerular cells. However, also in this model, YAP was detected in some glomeruli in PECs within lesions of *cd44–/–* mice (*Thy-1.1* tg *cd44–/–*; arrow; **B**). Pphospho-STAT3 and CD44 double immunostaining on WT kidney sections of the NTS model (**C**) and the anti-Thy-1.1 model (**D**). Phospho-STAT3 was detected in tubular cells and cells in the interstitium (**C**, **D**, arrowheads) but not in glomeruli or CD44-positive PECs (**C**, **D**, arrows). Bar = 50 μm.

Supplementary material is linked to the online version of the paper at www.kidney-international.org.

REFERENCES

1. Pavenstadt H, Kriz W, Kretzler M. Cell biology of the glomerular podocyte. *Physiol Rev*. 2003;83:253–307.
2. Kreidberg JA. Podocyte differentiation and glomerulogenesis. *J Am Soc Nephrol*. 2003;14:806–814.
3. Ohse T, Chang AM, Pippin JW, et al. A new function for parietal epithelial cells: a second glomerular barrier. *Am J Physiol Renal Physiol*. 2009;297:F1566–F1574.
4. Smeets B, Uhlig S, Fuss A, et al. Tracing the origin of glomerular extracapillary lesions from parietal epithelial cells. *J Am Soc Nephrol*. 2009;20:2604–2615.
5. Bariety J, Bruneval P. Activated parietal epithelial cells or dedifferentiated podocytes in FSGS: Can we make the difference? *Kidney Int*. 2006;69:194.
6. Gibson IW, Downie I, Downie TT, et al. The parietal podocyte: a study of the vascular pole of the human glomerulus. *Kidney Int*. 1992;41:211–214.
7. Schulte K, Berger K, Boor P, et al. Origin of parietal podocytes in atubular glomeruli mapped by lineage tracing. *J Am Soc Nephrol*. 2014;25:129–141.
8. Ronconi E, Sagrinati C, Angelotti ML, et al. Regeneration of glomerular podocytes by human renal progenitors. *J Am Soc Nephrol*. 2009;20:322–332.
9. Sagrinati C, Netti GS, Mazzinghi B, et al. Isolation and characterization of multipotent progenitor cells from the Bowman's capsule of adult human kidneys. *J Am Soc Nephrol*. 2006;17:2443–2456.
10. Smeets B, Kuppe C, Sicking EM, et al. Parietal epithelial cells participate in the formation of sclerotic lesions in focal segmental glomerulosclerosis. *J Am Soc Nephrol*. 2011;22:1262–1274.
11. Fatima H, Moeller MJ, Smeets B, et al. Parietal epithelial cell activation marker in early recurrence of FSGS in the transplant. *Clin J Am Soc Nephrol*. 2012;7:1852–1858.
12. Smeets B, Moeller MJ. Parietal epithelial cells and podocytes in glomerular diseases. *Semin Nephrol*. 2012;32:357–367.
13. Sheerin NS, Springall T, Carroll MC, et al. Protection against anti-glomerular basement membrane (GBM)-mediated nephritis in C3- and C4-deficient mice. *Clin Exp Immunol*. 1997;110:403–409.
14. Boucher A, Droz D, Adafer E, et al. Relationship between the integrity of Bowman's capsule and the composition of cellular crescents in human crescentic glomerulonephritis. *Lab Invest*. 1987;56:526–533.
15. Ophascharoensuk V, Pippin JW, Gordon KL, et al. Role of intrinsic renal cells versus infiltrating cells in glomerular crescent formation. *Kidney Int*. 1998;54:416–425.
16. Nagata M, Hattori M, Hamano Y, et al. Origin and phenotypic features of hyperplastic epithelial cells in collapsing glomerulopathy. *Am J Kidney Dis*. 1998;32:962–969.
17. Dijkman HB, Weening JJ, Smeets B, et al. Proliferating cells in HIV and pamidronate-associated collapsing focal segmental glomerulosclerosis are parietal epithelial cells. *Kidney Int*. 2006;70:338–344.
18. Suzuki T, Matsusaka T, Nakayama M, et al. Genetic podocyte lineage reveals progressive podocytopenia with parietal cell hyperplasia in a murine model of cellular/collapsing focal segmental glomerulosclerosis. *Am J Pathol*. 2009;174:1675–1682.
19. Dijkman H, Smeets B, van der Laak J, et al. The parietal epithelial cell is crucially involved in human idiopathic focal segmental glomerulosclerosis. *Kidney Int*. 2005;68:1562–1572.
20. Smeets B, Angelotti ML, Rizzo P, et al. Renal progenitor cells contribute to hyperplastic lesions of podocytopathies and crescentic glomerulonephritis. *J Am Soc Nephrol*. 2009;20:2593–2603.

21. Kuppe C, Grone HJ, Ostendorf T, et al. Common histological patterns in glomerular epithelial cells in secondary focal segmental glomerulosclerosis. *Kidney Int*. 2015;88:990–998.
22. Shankland SJ, Smeets B, Pippin JW, et al. The emergence of the glomerular parietal epithelial cell. *Nat Rev Nephrol*. 2014;10:158–173.
23. Cichy J, Pure E. The liberation of CD44. *J Cell Biol*. 2003;161:839–843.
24. Sicking EM, Fuss A, Uhlig S, et al. Subtotal ablation of parietal epithelial cells induces crescent formation. *J Am Soc Nephrol*. 2012;23:629–640.
25. Nakamura H, Kitazawa K, Honda H, et al. Roles of and correlation between alpha-smooth muscle actin, CD44, hyaluronic acid and osteopontin in crescent formation in human glomerulonephritis. *Clin Nephrol*. 2005;64:401–411.
26. Florquin S, Nunziata R, Claessen N, et al. CD44 expression in IgA nephropathy. *Am J Kidney Dis*. 2002;39:407–414.
27. Drew AF, Tucker HL, Liu H, et al. Crescentic glomerulonephritis is diminished in fibrinogen-deficient mice. *Am J Renal Physiol*. 2001;281: F1157–F1163.
28. Kuppe C, van Roeyen C, Leuchtle K, et al. Investigations of glucocorticoid action in GN. *J Am Soc Nephrol*. 2017;28:1408–1420.
29. Kabgani N, Grigoleit T, Schulte K, et al. Primary cultures of glomerular parietal epithelial cells or podocytes with proven origin. *PLoS One*. 2012;7.
30. Cai YI, Sich M, Beziau A, et al. Collagen distribution in focal and segmental glomerulosclerosis: an immunofluorescence and ultrastructural immunogold study. *J Pathol*. 1996;179:188–196.
31. Lensen JFM, van der Vlag J, Versteeg EMM, et al. Differential expression of specific dermatan sulfate domains in renal pathology. *Plos One*. 2015;10.
32. Eng DG, Sunseri MW, Kaverina NV, et al. Glomerular parietal epithelial cells contribute to adult podocyte regeneration in experimental focal segmental glomerulosclerosis. *Kidney Int*. 2015;88:999–1012.
33. Lee JL, Wang MJ, Chen JY. Acetylation and activation of STAT3 mediated by nuclear translocation of CD44. *J Cell Biol*. 2009;185:949–957.
34. Zhang YC, Xia HW, Ge XJ, et al. CD44 acts through RhoA to regulate YAP signaling. *Cell Signal*. 2014;26:2504–2513.
35. Roeder SS, Barnes TJ, Lee JS, et al. Activated ERK1/2 increases CD44 in glomerular parietal epithelial cells leading to matrix expansion. *Kidney Int*. 2017;91:896–913.
36. Le Hir M, Besse-Eschmann V. A novel mechanism of nephron loss in a murine model of crescentic glomerulonephritis. *Kidney Int*. 2003;63: 591–599.
37. Assmann KJ, Tangelder MM, Lange WP, et al. Anti-GBM nephritis in the mouse: severe proteinuria in the heterologous phase. *Virchows Arch A Pathol Anat Histopathol*. 1985;406:285–299.
38. Holdsworth SR, Neale TJ, Wilson CB. Abrogation of macrophage-dependent injury in experimental glomerulonephritis in the rabbit. Use of an antimacrophage serum. *J Clin Invest*. 1981;68:686–698.
39. Rops AL, Gotte M, Baselmans MH, et al. Syndecan-1 deficiency aggravates anti-glomerular basement membrane nephritis. *Kidney Int*. 2007;72:1204–1215.
40. Atkins RC, Holdsworth SR, Glasgow EF, et al. The macrophagen in human rapidly progressive glomerulonephritis. *Lancet*. 1976;1:830–832.
41. Bariety J, Bruneval P, Meyrier A, et al. Podocyte involvement in human immune crescentic glomerulonephritis. *Kidney Int*. 2005;68:1109–1119.
42. Duffield JS, Tipping PG, Kipari T, et al. Conditional ablation of macrophages halts progression of crescentic glomerulonephritis. *Am J Pathol*. 2005;167:1207–1219.
43. Nikolic-Paterson DJ, Atkins RC. The role of macrophages in glomerulonephritis. *Nephrol Dial Transplant*. 2001;16(suppl 5):S3–S7.
44. Rouschop KMA, Sewnath ME, Claessen N, et al. CD44 deficiency increases tubular damage but reduces renal fibrosis in obstructive nephropathy. *J Am Soc Nephrol*. 2004;15:674–686.
45. Rops ALWMM, Loeven MA, van Gemst JJ, et al. Modulation of heparan sulfate in the glomerular endothelial glycocalyx decreases leukocyte influx during experimental glomerulonephritis. *Kidney Int*. 2014;86: 932–942.
46. Peired A, Angelotti ML, Ronconi E, et al. Proteinuria impairs podocyte regeneration by sequestering retinoic acid. *J Am Soc Nephrol*. 2013;24: 1756–1768.
47. Konieczny A, Czyzewska-Buczynska A, Ryba M, et al. Expression of cell membrane antigens in cells excreted in the urinary sediment predicts progression of renal disease in patients with focal segmental glomerulosclerosis. *Am J Nephrol*. 2015;42:35–41.
48. Osada S, Ebihara I, Nakamura T, et al. In situ hybridization of type I collagen mRNA in puromycin aminonucleoside-induced glomerulosclerosis. *Exp Nephrol*. 1995;3:40–48.
49. Minto AW, Fogel MA, Natori Y, et al. Expression of type I collagen mRNA in glomeruli of rats with passive Heymann nephritis. *Kidney Int*. 1993;43: 121–127.
50. Yoshioka K, Tohda M, Takemura T, et al. Distribution of type I collagen in human kidney diseases in comparison with type III collagen. *J Pathol*. 1990;162:141–148.
51. Rouschop KMA, Roelofs JJTH, Claessen N, et al. Protection against renal ischemia reperfusion injury by CD44 disruption. *J Am Soc Nephrol*. 2005;16:2034–2043.
52. Smeets B, Te Loeke NA, Dijkman HB, et al. The parietal epithelial cell: a key player in the pathogenesis of focal segmental glomerulosclerosis in Thy-1.1 transgenic mice. *J Am Soc Nephrol*. 2004;15:928–939.
53. Scholz J, Lukacs-Kornek V, Engel DR, et al. Renal dendritic cells stimulate IL-10 production and attenuate nephrotoxic nephritis. *J Am Soc Nephrol*. 2008;19:527–537.
54. Raats CJI, Bakker MAH, Hoch W, et al. Differential expression of agrin in renal basement membranes as revealed by domain-specific antibodies. *J Biol Chem*. 1998;273:17832–17838.